The Frequency Behavior of Stripline Circulator Junctions

SEVIĞ AYTER AND YALÇIN AYASLI

Abstract—**The frequency dependence of the circulation equations for Y-junction stripline and microstrip circulators is investigated, and a new set of design curves is generated for the frequency-independent forms of the circulation condition's roots for both below- and above-resonance cases. Using this new set of curves, the wide-band design predicted by Wu and Rosenbaum and Bosma's narrow-band design are analyzed and compared. Quantitative arguments for the effect of the junction parameters on the bandwidth are given. To support the arguments, the theoretical junction performance of the 7–15 GHz "continuous tracking" circulator reported by Wu and Rosenbaum is calculated and compared with the theoretical performance of a 2–4 GHz circulator junction designed using the same method. Experimental results also are presented for the 2–4 GHz design.**

An analysis for the effect of the ferrite thickness on impedance matching is also included.

I. Introduction

THE ANALYSIS of stripline Y-junction circulators generally employs Bosma's Green-function method to solve for the junction fields. This theory leads to two circulation equations which must be satisfied simultaneously for ideal circulation. These circulation equations are reviewed and then reformulated, generating a new set of design curves for both below- and above-resonance cases in order to bring out the frequency dependence in an explicit manner. These new design curves provide more information on the frequency behavior of the junction. They are especially useful in understanding the effect of the junction parameters on the intrinsic bandwidth of the wide-band designs.

II. General Behavior of the Circulation Equations

The first and second circulation equations for a stripline or microstrip Y-junction circulator with the junction geometry (shown in Fig. 1) are given as [1], [2]

$$P = \frac{M(M^2 - 3N^2)}{M^2 + N^2} \tag{1}$$

and

$$Q = \frac{N(3M^2 - N^2)}{M^2 + N^2} \tag{2}$$

Manuscript received March 11, 1977, revised July 18, 1977.

S. Ayter was with the Department of Electrical Engineering, Middle East Technical University, Ankara, Turkey. He is now with the Department of Electrical Engineering, Stanford University, Stanford, CA 94305.

Y. Ayaslı is with the Department of Electrical Engineering, Middle East Technical University, Ankara, Turkey.

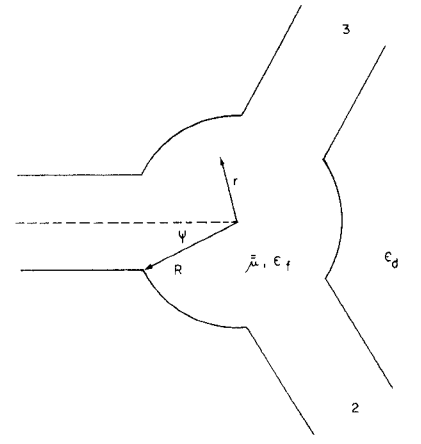

Fig. 1 Junction configuration.

where

$$P = \frac{\psi}{2}\frac{J_0(x)}{J_0'(x)} + \sum_{n=1}^{\infty}\left(\frac{\sin^2 n\psi}{n^2\psi}\right)\frac{J_n(x)J_n'(x)}{D_n}$$

$$Q = \frac{\pi Z_d}{2Z_{\text{eff}}}$$

$$M = \frac{\psi}{2}\frac{J_0(x)}{J_0'(x)} + \sum_{n=1}^{\infty}\left(\frac{\sin^2 n\psi}{n^2\psi}\right)\frac{J_n(x)J_n'(x)}{D_n}\cos(2n\psi/3)$$

$$N = \sum_{n=1}^{\infty}\left(\frac{\sin^2 n\psi}{n^2\psi}\right)\frac{J_n(x)J_n'(x)}{D_n}(n\kappa/\mu x)\sin(2n\psi/3)$$

$$D_n = [J_n'(x) - (n/x)|\kappa/\mu|J_n(x)] \cdot [J_n'(x) + (n/x)|\kappa/\mu|J_n(x)]$$

$x = kR$

$Z_d = 120\pi/(\varepsilon_d)^{1/2}$ ohms

= wave impedance of the surrounding medium

$Z_{\text{eff}} = (\mu_0\mu_{\text{eff}}/\varepsilon_0\varepsilon_f)^{1/2}$

= intrinsic wave impedance of the ferrite

$J_n(x)$ = Bessel function of the first kind with order n

$J_n'(x)$ = derivative of $J_n(x)$ with respect to its argument

μ,κ = Polder tensor elements of the ferrite

$\mu_{\text{eff}} = (\mu^2 - \kappa^2)/\mu$

= effective permeability of the ferrite

$k = (\omega/c)(\mu_{\text{eff}}\varepsilon_f)^{1/2}$

= radial wave propagation constant.

0018-9480/78/0300-0197$00.75

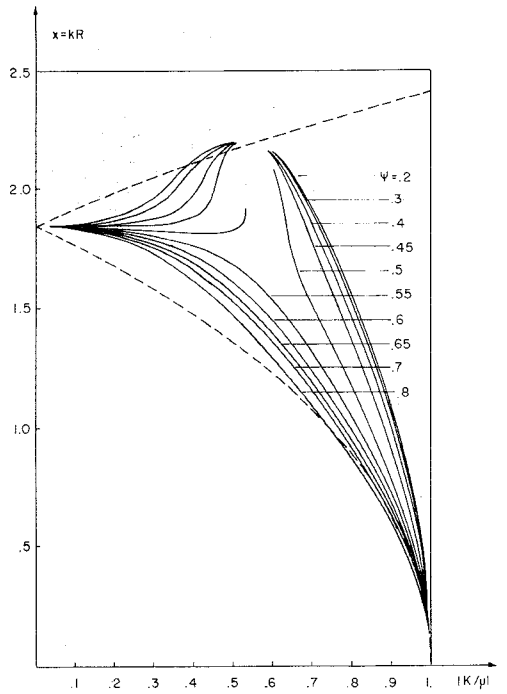

Fig. 2. Roots of the first circulation equation for various coupling angles.

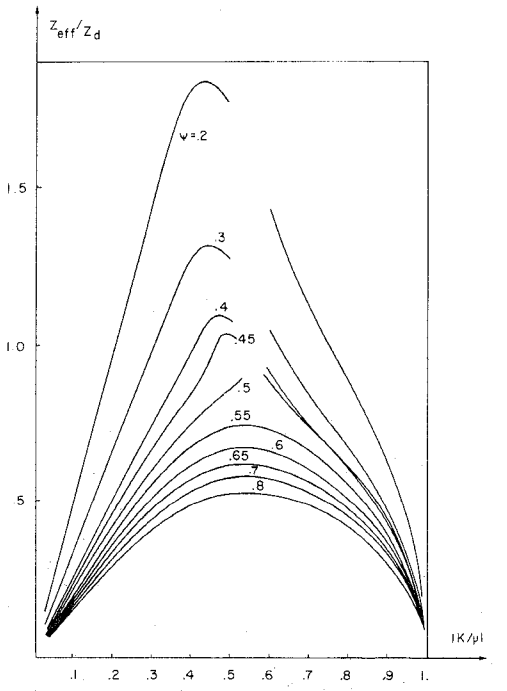

Fig. 3. Roots of the second circulation equation for various coupling angles.

In order to obtain the ideal circulation conditions of the junction, (1) and (2) must be solved simultaneously. They are derived by requiring infinite isolation between the isolated ports of the junction [3].

The solution of the first and second circulation equations are shown in Figs. 2 and 3, respectively. These curves agree well with those given by Wu and Rosenbaum [1]. For a small region bounded by $0.2 < \psi < 0.5$ and $0.5 < |\kappa/\mu| < 0.6$, the first and second circulation equations have multiroots, and this region is left blank. The dashed lines in Fig. 2 correspond to the first root pair of the resonance equation, $D_n = 0$, for $n = 1$. The roots are found by means of Mueller's iteration scheme of successive bisection and inverse parabolic interpolation [4].

III. Frequency Dependence of the Junction Circulator

The parameters k, Z_{eff}, and $|\kappa/\mu|$ are all frequency dependent quantities, and, therefore, Figs. 2 and 3 do not explain how the circulation action is affected by the frequency variations. The equations for κ, μ, μ_{eff}, k, Z_{eff}/Z_d are

$$\kappa = -\frac{f_m f}{(f_z^2 - f^2)} \tag{3}$$

$$\mu = 1 + \frac{f_m f_z}{(f_z^2 - f^2)} \tag{4}$$

$$\mu_{\text{eff}} = [1 - (\kappa/\mu)^2]\mu \tag{5}$$

$$k = (2\pi f/c)(\varepsilon_f \mu_{\text{eff}})^{1/2} \tag{6}$$

$$Z_{\text{eff}}/Z_d = (\mu_{\text{eff}} \varepsilon_d/\varepsilon_f)^{1/2} \tag{7}$$

where

f = operation frequency;

$f_z = (2.8H_0)$ MHz for H_0 measured in Oe;

$f_m = (2.8x4\pi M_s)$ MHz for $4\pi M_s$ measured in G.

The frequency dependence of the circulation action must be investigated for below- and above-resonance operations separately.

Case 1: Below-Resonance Operation

For below-resonance operation, the following condition must be satisfied:

$$f \gg f_m + f_z. \tag{8}$$

When $f_z \ll f_m$, i.e., the ferrite is just saturated, the ferrite and junction parameters can be approximated as

$$\kappa \simeq f_m/f \tag{9}$$

$$\mu \simeq 1 \tag{10}$$

$$|\kappa/\mu| \simeq f_m/f \tag{11}$$

$$\mu_{\text{eff}} \simeq 1 - |\kappa/\mu|^2 \tag{12}$$

$$k \simeq (2\pi f_m/c)(\varepsilon_f)^{1/2}(1 - |\kappa/\mu|^2)^{1/2}/|\kappa/\mu| \tag{13}$$

and

$$Z_{\text{eff}}/Z_d \simeq (\varepsilon_d/\varepsilon_f)^{1/2}(1 - |\kappa/\mu|^2)^{1/2}. \tag{14}$$

The first circulation equation solutions give kR as a function of $|\kappa/\mu|$ and ψ, that is;

$$kR = F_1[|\kappa/\mu|, \psi]. \tag{15}$$

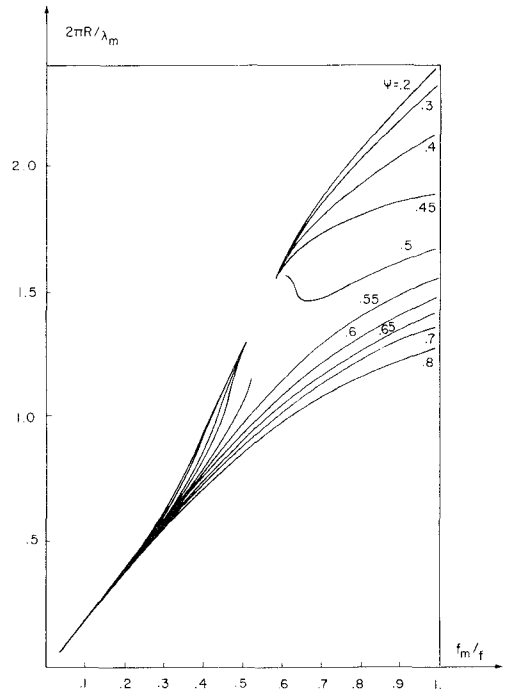

Fig. 4. Frequency-independent form of the roots of the first circulation equation under below-resonance conditions.

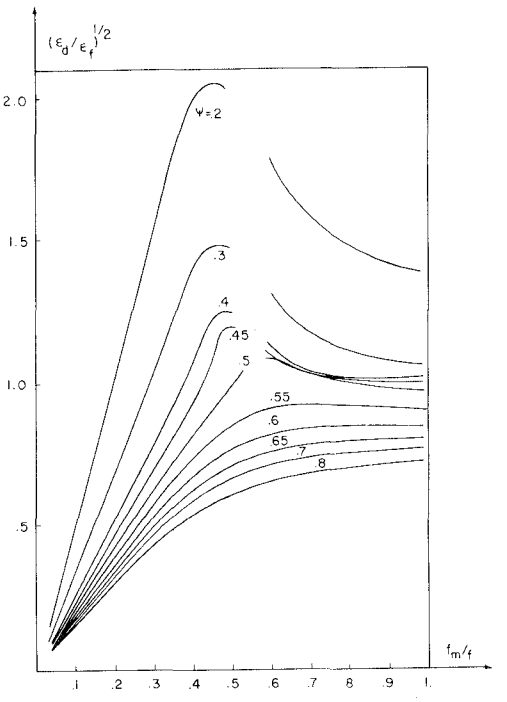

Fig. 5. Frequency-independent form of the roots of the second circulation equation under below-resonance conditions.

Using (11) and (13), (15) can be rewritten as

$$2\pi R/\lambda_m = \frac{(f_m/f)}{(1-(f_m/f)^2)^{1/2}} F_1[(f_m/f), \psi] \tag{16}$$

where $\lambda_m \equiv c/(\sqrt{\varepsilon_f}\, f_m)$ is a constant depending on the ferrite used.

The second circulation equation is of the form

$$Z_{\text{eff}}/Z_d = F_2(|\kappa/\mu|, \psi) \tag{17}$$

and using (11) and (14), it can be rewritten as

$$(\varepsilon_d/\varepsilon_f)^{1/2} = \frac{F_2[(f_m/f), \psi]}{[1-(f_m/f)^2]^{1/2}}. \tag{18}$$

Equation (16) gives the required disk-radius variation and (18) gives the required junction dielectric constant variation with frequency. These equations are plotted in Figs. 4 and 5 using the solutions of the circulation equations given in Figs. 2 and 3. Since $R, \lambda_m, \varepsilon_f$, and ε_d are not functions of the frequency, the curves must stay constant over the bandwidth of interest if broadband circulation action is required. In Fig. 5 the curves stay almost constant for $\psi > 0.4$ and $0.5 < f_m/f < 1$, and, therefore, over approximately the octave bandwidth of $f_z + f_m < f < 2f_m$, the second circulation equation can be satisfied.

The first circulation equation can also be satisfied over the same frequency range. The best choice for ψ seems to be around 0.5 rad. For this choice, at the center frequency of $f_0 = 1.5f_m$, the variation in R/λ_m ratio is less than ∓ 10 percent when the frequency is changed within the octave band specified above. Then Fig. 5 gives the optimum value for $(\varepsilon_d/\varepsilon_f)$ ratio corresponding to $\psi = 0.5$ as unity.

Unity ratio for the dielectric constants can be achieved by inserting the ferrite disk into a hole in the substrate of a dielectric constant equal to that of the ferrite, or using the ferrite itself as the substrate and biasing only the junction region. Both methods are equally applicable in practice [5], [1]. When a smaller dielectric constant is used for the surrounding medium, one must increase the coupling angle (see Fig. 5), but available intrinsic bandwidth decreases in this case (see Fig. 4).

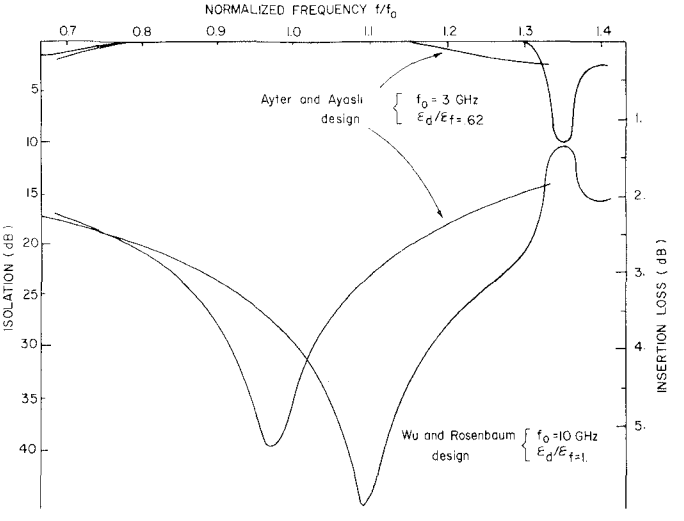

Fig. 6. Calculated isolation and insertion loss for the "continuous-tracking" circulators for $\varepsilon_d/\varepsilon_f = 1.0$ and $\varepsilon_d/\varepsilon_f = 0.62$.

To illustrate this point more clearly, junction parameters for the "continuous-tracking circulator" designed by Wu and Rosenbaum are calculated, and among them junction isolation and insertion loss are plotted in Fig. 6. This should be an example to optimum design with $\varepsilon_d/\varepsilon_f = 1$. For an

application of the design to an $\varepsilon_d/\varepsilon_f < 1$ case, a circulator junction at 3 GHz with $\varepsilon_d/\varepsilon_f = 0.62$ is designed. The junction parameters for this circulator are also calculated, and isolation and insertion losses are shown on the same figure. The decrease in the intrinsic bandwidth is evident. It must be noted that in the theoretical analysis of the junction designed by Wu and Rosenbaum, the junction parameters, in addition to those shown in Fig. 6, all showed the sudden deterioration around 13.4 GHz. An explanation for this behavior may be found by examining the frequency independent form of the roots of the first circulation equation in Fig. 4. For ψ around 0.5 (for Wu and Rosenbaum $\psi = 0.52$) there is a sudden hump on the curve, which should be responsible for the hump of the junction behavior. Wu and Rosenbaum noticed a sudden deterioration around 13.2 GHz in their experimental results for the insertion loss but attributed it to other causes.

Case 2: Above-Resonance Operation

For above-resonance operation, f_z must be larger than f. When $f_z^2 \gg f^2$, the ferrite and junction parameters can be approximated as

$$\kappa \simeq -\frac{f_m}{f_z^2} f \tag{19}$$

$$\mu \simeq 1 + \frac{f_m}{f_z} \tag{20}$$

$$|\kappa/\mu| \simeq \frac{f_m}{(f_m + f_z) f_z} f \tag{21}$$

$$\mu_{\text{eff}} \simeq \left(1 + \frac{f_m}{f_z}\right)[1 - (\kappa/\mu)^2] \tag{22}$$

$$k \simeq \frac{2\pi\sqrt{\varepsilon_f}}{c} \frac{f_z^{1/2}(f_m + f_z)^{3/2}}{f_m} |\kappa/\mu|[1 - (\kappa/\mu)^2]^{1/2} \tag{23}$$

and

$$Z_{\text{eff}}/Z_d \simeq \left(1 + \frac{f_m}{f_z}\right)^{1/2} (\varepsilon_d/\varepsilon_f)^{1/2}[1 - (\kappa/\mu)^2]^{1/2}. \tag{24}$$

Following the same steps as in the previous case, a constant C_a can be defined as

$$C_a \equiv \frac{2\pi\sqrt{\varepsilon_f}}{c} f_z^{1/2} \frac{(f_m + f_z)^{3/2}}{f_m} \tag{25}$$

such that

$$C_a R = \frac{F_1[|K/\mu|, \psi]}{|K/\mu|[1 - (K/\mu)^2]^{1/2}} \tag{26}$$

can be written for the first circulation condition. The second circulation condition, on the other hand, can be rearranged as

$$\left(1 + \frac{f_m}{f_z}\right)^{1/2} (\varepsilon_d/\varepsilon_f)^{1/2} = \frac{F_2[|\kappa/\mu|, \psi]}{[1 - (\kappa/\mu)^2]^{1/2}}. \tag{27}$$

Since $|\kappa/\mu| \simeq [f_m/(f_m + f_z)](f/f_z)$ and $f_z^2 \gg f^2$, the above results are valid only for small $|\kappa/\mu|$. Usually f_m and f_z are of the same order. If $f_z \geq 3f_{\max}$ is taken as a rule for smallness, where $f_{\max}$ is the maximum value of the operation frequency, it is seen that the above analysis is valid for $|\kappa/\mu| < 0.2$. Equations (26) and (27) are plotted in Figs. 7 and 8, respectively. These figures show that no inherent broadband circulation of the junction exists for above-resonance circulators. In fact when $|\kappa/\mu|$ is small, the circulation equation roots are close to the roots of the first order resonance equation and approximating each series expression by only the $n = 1$ term is quite valid. Bosma [3]

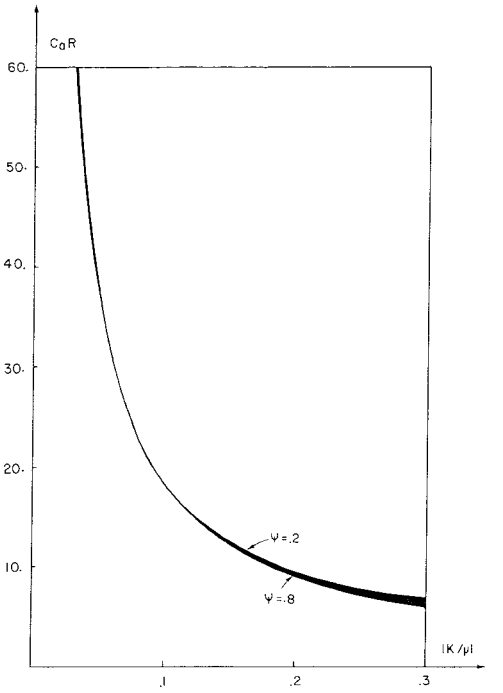

Fig. 7. Frequency-independent form of the roots of the first circulation equation under above-resonance operation.

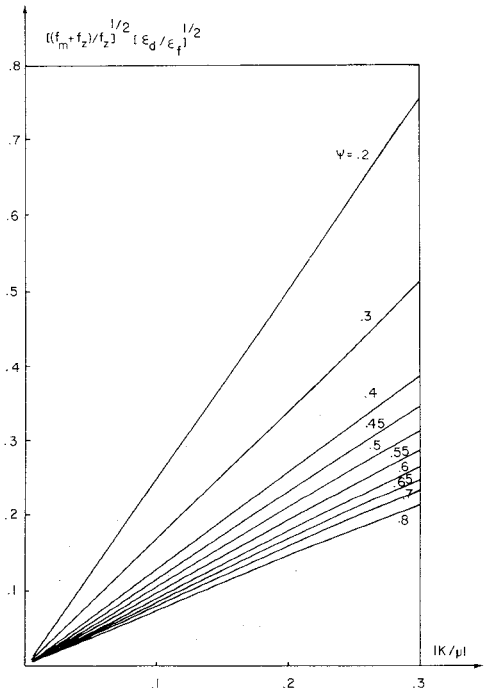

Fig. 8. Frequency-independent form of the roots of the second circulation equation under above-resonance conditions.

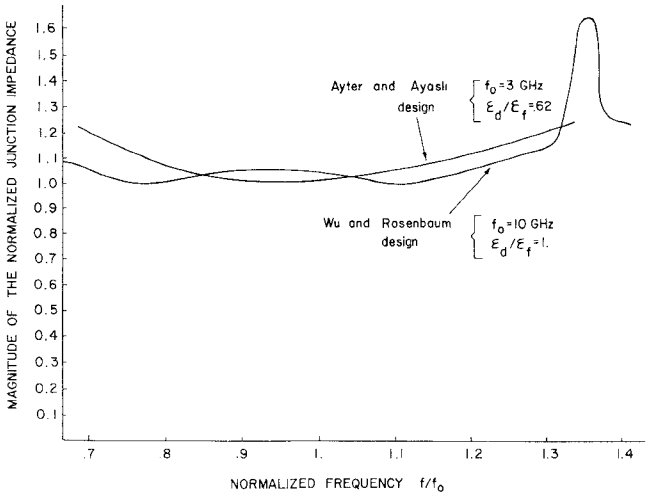

Fig. 9. The magnitude of the calculated junction impedance normalized with respect to the characteristic impedance of the stripline at the edge of the disk under perfect circulation.

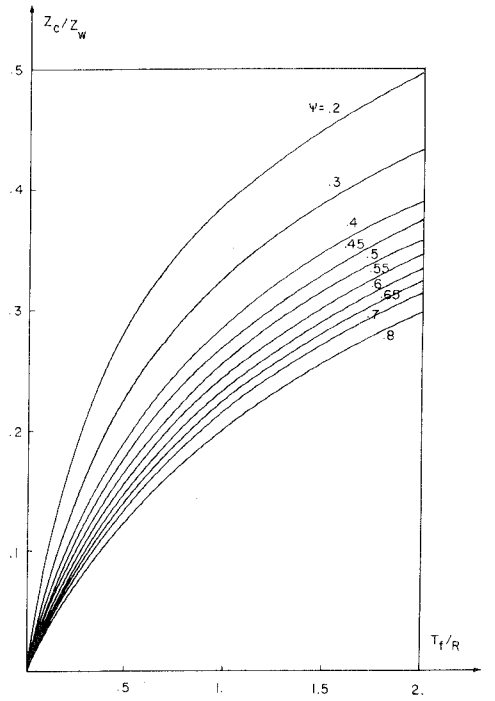

Fig. 10. The geometric factor of the stripline at the edge of the disk as a function of the disk thickness T_f over radius ratio for various coupling angles.

calculated the relative bandwidth approximating the Green's function by only its first term and found the fractional bandwidth as $\Delta f/f_0 = 2.9(|\kappa/\mu|)\rho_{\max}$ where f_0 is the center frequency and $\rho_{\max}$ is the maximum allowable value of the input reflection coefficient. For $f_0 = 450$ MHz and $\rho_{\max} = 0.1$, he found 3.2 percent fractional bandwidth. Therefore, if broadband operation of the above resonance circulator is required, external matching techniques must be used [3], [6].

The first order approximation also reduces the first and second circulation equations to

$$kR = 1.84 \tag{28}$$

and

$$\frac{\sin^2 \psi}{\psi} = \frac{\pi}{\sqrt{3}} \frac{1}{1.84} \frac{Z_d}{Z_{\text{eff}}} |\kappa/\mu|. \tag{29}$$

Equation (28) shows that the disk radius R is not a function of the coupling angle ψ for above-resonance circulators. This result agrees with Fig. 7. Also (29) gives Z_{eff}/Z_d as a linear function of $|\kappa/\mu|$, and this is an accurate approximation of Fig. 8 for small $|\kappa/\mu|$. Therefore, (28) and (29) are quite sufficient for the design of above-resonance circulators.

IV. Impedance-Matching Considerations for the Wide-Band Design

The junction impedance remains fairly constant over an octave bandwidth for the wide-band designs as shown in Fig. 9. However, the problem of matching this impedance to the impedance of the feeding transmission lines still remains. The effect of the ferrite thickness on this impedance is discussed in this section.

The analysis presented so far does not include the ferrite thickness as a parameter since the fields were assumed to be z-invariant. The most important factor in determining the ferrite thickness is the characteristic impedance of the stripline at the edge of the junction. This impedance is also the input impedance of the circulator junction under circulation conditions. Since the main objective for broad-band circulators is to match the input impedance at the edge of the disk (which stays fairly constant over the bandwidth of interest) to the external feed lines, it is desirable to obtain an input impedance as near as possible to the impedance of the feedlines (usually 50 Ω), for a relatively easy broad-band matching procedure. There is an extensive literature on the general topic of triplate stripline, and much of this is devoted to attempts to derive accurate but simple approximation formulas for the characteristic impedance. For zero-thickness triplate striplines, Rochelle [7] gave the following equation for the characteristic impedance Z_c which is said to be highly accurate for both wide ($w/b > 0.5$) and narrow ($w/b < 0.5$) striplines with maximum inaccuracy of 5 percent on the transition region ($w/b \simeq 0.5$), where w is the width of the stripline, and b is the distance between the ground plates;

$$Z_c = \frac{Z_w}{\pi}\left\{\frac{1}{u}\tan^{-1} u + 0.25 \ln (1 + u^{-2}) - 0.25u^{-2} \ln (1 + u^2)\right\} \tag{30}$$

where

$$u = 2w/b, \tag{31}$$

$$Z_w = 376.687/\sqrt{\varepsilon_d}\ \Omega \tag{32}$$

and ε_d is the relative dielectric constant of the medium between the ground plates. The width of the stripline at the edge of the disk is

$$w = 2R \sin \psi. \tag{33}$$

Using (30) and (33) and taking ψ as a parameter, a family of curves for the geometric factor of the triplate stripline, i.e., Z_c/Z_w at the edge of the disk, has been generated and is presented in Fig. 10. This family of curves proved to be very

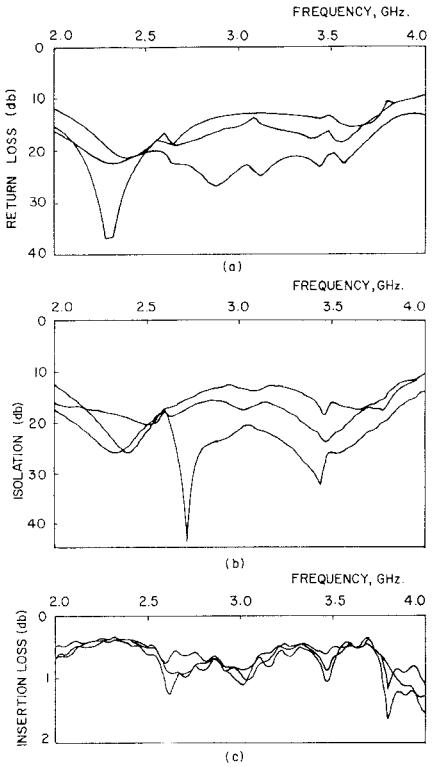

Fig. 11. Experimental performance of the "continuous-tracking" 2–4-GHz circulator. (a) Return loss. (b) Isolation. (c) Insertion loss.

useful, not only for choosing the ferrite thickness, but also for investigating the limits of the characteristic impedance that can be obtained at the edge of the junction for a given ε_d. The limitation comes from the fact that the method of analysis depends on the basic assumption of TEM-wave propagation in striplines. The suppression of the higher order modes can be achieved if the distances between the ground plates measure less than half the wavelength of the waves propagating in the stripline [8]. Therefore, there is an upper bound for the ferrite disk thickness, and thus there is an upper bound for a given ψ and ε_d on the maximum Z_c that can be achieved.

V. Experimental Results

The 2–4-GHz circulator which has the theoretical junction performance shown in Fig. 6 was realized using TDK-Y3 Y-A1 garnet material which has a saturation magnetization of 750 G. The disk radius is 7.5 mm, and the junction coupling angle is $\psi = 0.65$ rad. The biasing magnet was of TDK-FB2 material. The circulator is matched by a "triangular taper" [9].

The experimental performance of the designed circulator with 24-mm matching taper sections is given in Fig. 11, with each port measured sequentially. On the average, better than 15-dB isolation and return loss, and lower than 1-dB insertion loss are obtained over the octave bandwidth. However, the circulator characteristics do not track well from port to port because the center conductor was hand cut and did not have a perfect symmetry. Better machining techniques should improve the performance. To point out that no extensive matching network need be developed to increase the bandwidth, no alignment or tuning was done to obtain better tracking between ports or to decrease insertion loss.

VI. Conclusion

The design criteria for the Y-junction stripline circulators are reviewed and reformulated in a frequency independent form. This new set of design curves thus generated shows that "the continuous-tracking" circulator does have a large intrinsic bandwidth. The effect of the junction parameters on this bandwidth is investigated using these curves, and the conclusions are supported by the theoretical and experimental data obtained on two wide-band designs. These theoretical and experimental results provide conclusive evidence confirming the validity of the wide-band design.

Acknowledgment

The authors wish to thank S. Sekine of TDK Electronics Co., Ltd., for supplying the permanent magnets.

References

[1] Y. S. Wu and F. J. Rosenbaum, "Wide-band operation of microstrip circulators," *IEEE Trans. Microwave Theory Tech.*, vol. MTT-22, pp. 849–856, Oct. 1974.
[2] J. B. Davies and P. Cohen, "Theoretical design of symmetrical junction stripline circulators," *IEEE Trans. Microwave Theory Tech.*, vol. MTT-11, pp. 506–512, Nov. 1963.
[3] H. Bosma, "On stripline Y-circulation at UHF," *IEEE Trans. Microwave Theory Tech.*, vol. MTT-12, pp. 61–72, Jan. 1964.
[4] *Scientific Subroutine Package, Mathematics: Roots of Nonlinear Equations*, IBM, pp. 217–219.
[5] D. J. Massé, "Broadband microstrip junction circulators," *Proc. IEEE*, vol. 56, pp. 352–353, Mar. 1968.
[6] Y. Konishi, "Lumped element Y-circulator," *IEEE Trans. Microwave Theory Tech.*, vol. MTT-13, pp. 852–864, Nov. 1965.
[7] J. M. Rochelle, "Approximations for the symmetrical parallel strip transmission line," *IEEE Trans. Microwave Theory Tech.*, vol. MTT-23, pp. 712–714, Aug. 1975.
[8] M. A. R. Gunston, *Microwave Transmission Line Impedance Data*. London, England: Van Nostrand Reinhold, 1972.
[9] R. E. Collin, *Foundations for Microwave Engineering*. New York: McGraw-Hill, 1966.